

Scintillator studies with MeV charged particle beams

M. Tuszewski

Los Alamos National Laboratory, Los Alamos, New Mexico 87545

S. J. Zweben

Princeton Plasma Physics Laboratory, Princeton, New Jersey 08544

(Received 10 February 1993; accepted for publication 7 May 1993)

Thin scintillators used as detectors of escaping fusion products in the TFTR tokamak are studied with Van de Graaf beams of 3-MeV protons and 3.5-MeV alphas. ZnS scintillators are found generally adequate for the D-D experiments performed up to now, marginal for near-term D-T experiments because the emitted light saturates at alpha fluxes greater than $10^{10} \text{ cm}^{-2} \text{ s}^{-1}$, and totally inadequate for future ignited plasmas. Other scintillators have been tested that have lower light efficiencies but much better properties at high fluxes. In particular, the P46 scintillator appears to be an excellent choice for future experiments.

I. INTRODUCTION

Studies of the light emitted by several thin scintillators exposed to Van de Graaf charged particle beams are presented. These studies aim at characterizing the ZnS scintillators used in the TFTR tokamak to detect escaping charged fusion products¹ and at identifying scintillators suitable for future D-T experiments. Preliminary studies with ZnS scintillators suggested a light saturation at high beam currents.² We extend and clarify these results in this article, and study scintillators that have better properties at high particle fluxes. In Sec. II, results on beam current density dependence, relative light efficiencies, time response, temperature effects, and radiation damage are presented. The implications of these results for future experiments and the most likely cause of the observed saturations are discussed in Sec. IV.

II. STUDIES WITH VAN DE GRAAF BEAMS

The experiments are done at the Los Alamos Ion Beam Facility in a vacuum chamber sketched in Fig. 1. Details of the experimental procedure have been given previously.² The only addition in Fig. 1 is that an iris of 0.5 cm diameter is placed in front of the light-collecting lens train to limit the intensity of the scintillator image on the photocathode of the photomultiplier tube. This is necessary to avoid a saturation of the tube output at high light levels that led to overestimates² of the scintillator nonlinearities. A linear PM tube response is now obtained over the entire intensity range of interest, when checked with various lamps and with a photometer.

Data are presented for four different scintillators referred as P11, P31, S2370, and P46. The P11 is a blue-emitting ZnS:Ag phosphor chosen for the first TFTR detectors.¹ It has the highest light efficiency, but only at low temperatures. The P31 is a green-emitting ZnS:Cu phosphor used in present TFTR experiments. These ZnS scintillators are widely used in oscilloscope and color television screens. Two yellow-green phosphors are also studied: the Sylvania 2370 is an yttrium vanadate ($\text{YVO}_4\text{:V:Dy}$) used in fluorescent lights and the P46 is an yttrium aluminum garnet ($\text{Y}_3\text{Al}_5\text{O}_{12}\text{:Ce}$) used in flying-

spot scanners. All the above phosphors are powders of 1–10 μm grain size and 10–20 μm average thickness deposited on quartz substrates ($2.5 \times 2.5 \times 0.1 \text{ cm}$).

A. Dependence on beam current density

The scintillators are oriented at $\varphi = 20^\circ$ as shown in Fig. 1. This choice for φ approximates TFTR experiments¹ in which charged fusion products are detected with incidence angles of 15° – 20° . Van de Graaf beam current scans are performed in the range 10^{-10} – 10^{-6} A . Most scans are made with 3-MeV protons and a few scans are made with 3.5-MeV alphas. These ions are the main light-producing fusion products in TFTR D-D and D-T experiments.¹ The results of the current scans are shown in Figs. 2–5 for the P11, P31, S2370, and P46 scintillators, respectively. Each data point records the light output of the scintillator in arbitrary units, from a 30–60 s exposure to a steady-state beam. All data are obtained with identical PM tube voltage (0.25 kV) and preamplifier gain (10^4). The symbols correspond to various impacted scintillator areas A , indicated on the figures. Beam apertures sketched in Fig. 1 are used to vary A , from 0.15 to 2.3 cm^2 . The hollow symbols refer to protons and the solid symbols refer to alphas. There are factor of two uncertainties in the absolute magnitude of

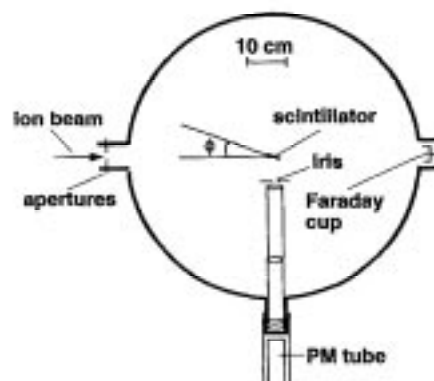


FIG. 1. Sketch of the Van de Graaf vacuum chamber and of the experimental apparatus.

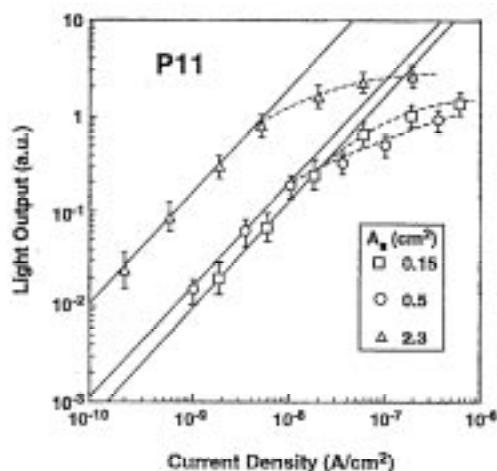


FIG. 2. Light output of the P11 scintillator as function of 3-MeV proton beam current density.

each data point due to beam fluctuations, to errors in the estimations of A_b , and to variations in the scintillator location that is impacted and associated variations in light collection.

The P11 scintillator has a linear light output up to $j \sim 8 \times 10^{-9} \text{ A/cm}^2$ and then saturates, as seen from Fig. 2. The onset of saturation corresponds to a proton flux $\Gamma = j/Z_e \sim 5 \times 10^{10} \text{ cm}^{-2} \text{ s}^{-1}$, where Z is the projectile atomic number. Each proton deposits $\Delta E = 1.9 \text{ MeV}$ into the scintillator powder, so that the onset also corresponds to a power density $P/A_b = \Delta E \Gamma \sim 15 \text{ mW/cm}^2$. The proton data of Fig. 3 show similar trends for the P31 scintillator, with a somewhat lower onset of saturation (about $5 \times 10^{-9} \text{ A/cm}^2$, $3 \times 10^{10} \text{ cm}^{-2} \text{ s}^{-1}$, and 10 mW/cm^2). The alpha data of Fig. 3 also show light saturation beyond $(3-4) \times 10^{-9} \text{ A/cm}^2$. This onset corresponds to $10^{10} \text{ cm}^{-2} \text{ s}^{-1}$ and to 6 mW/cm^2 since each alpha deposits 3.5

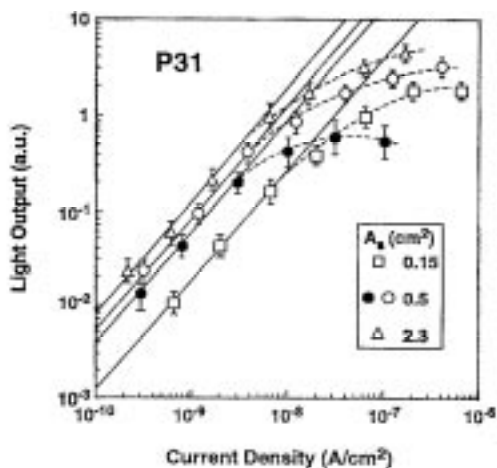


FIG. 3. Light output of the P31 scintillator as function of beam current density. The hollow symbols are for 3-MeV protons and the solid symbols are for 3.5-MeV alphas.

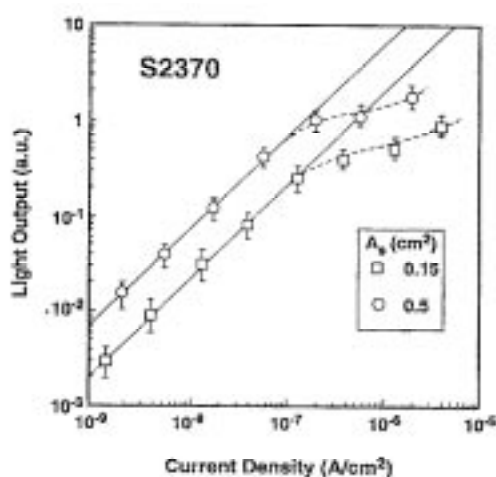


FIG. 4. Light output of the Sylvania 2370 scintillator as function of 3-MeV beam current density.

MeV into the scintillator powder. The S2370 data of Fig. 4 show light saturation at higher current densities, beyond about 10^{-7} A/cm^2 . Finally, the P46 data of Fig. 5 suggest a linear light output in all cases, up to the Van de Graaf upper limit of about 10^{-5} A/cm^2 .

B. Relative light efficiencies

The relative light efficiencies of the scintillators can be roughly extracted, at given current density within the linear response region, from the data of Figs. 2-5. The P11 and P31 scintillators have similar efficiencies, as seen from Figs. 2 and 3 and as already reported.² The S2370 and P46 scintillator also have similar light efficiencies, lower by factors of 10-30 relative to the ZnS scintillators. These estimates suffer from uncertainties in beam location and in ion energy deposited into the powder. In addition, the ZnS

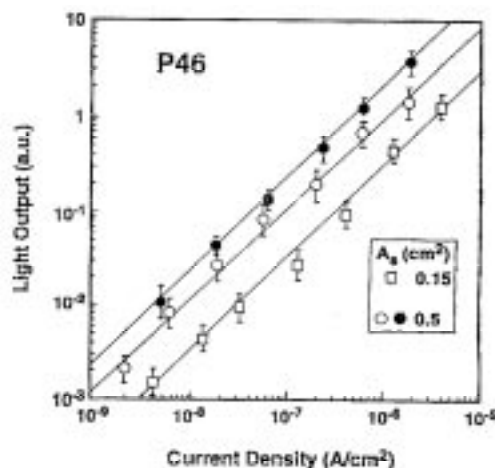


FIG. 5. Light output of the P46 scintillator as function of beam current density. The hollow symbols are for 3-MeV protons and the solid symbols are for 3.5-MeV alphas.

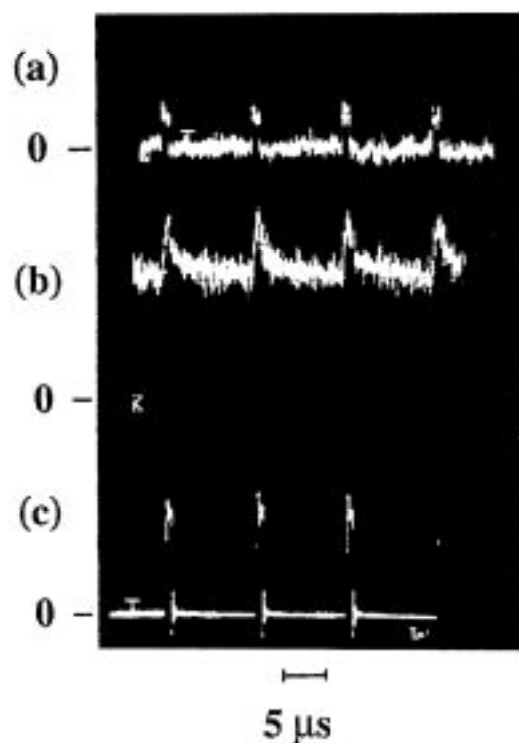


FIG. 6. Voltage traces showing (a) a chopped 3-MeV proton beam current, (b) the response of a Sylvania 2370 scintillator, and (c) the response of a P46 scintillator.

scintillators have a thin aluminum layer between phosphor powder and quartz substrate, unlike the P46 and S2370 scintillators. This aluminum layer reflects some of the emitted light and increases the scintillator brightness by about a factor of 1.7. The relative light efficiencies are more accurately assessed in separate experiments with a Curium alpha source and with scintillators without aluminum layer. The Curium source² is placed in the beam direction 2 cm in front of the scintillator. Measurements are taken in vacuum with the scintillators oriented at $\varphi=45^\circ$. Taking into account the spectral response of the PM tube, relative alpha light efficiencies of 1 for P11, 0.85 ± 0.05 for P31, 0.08 ± 0.01 for P46, and 0.06 ± 0.01 for S2370 scintillators are obtained.

The ratio of alpha to proton light output for a given scintillator is also of experimental interest. Such ratios can be obtained from Figs. 3 and 5, at fixed particle flux (j/Z) within the linear response. A ratio of about 1.5 is obtained from the P31 data of Fig. 3. This is consistent with the assumption that emitted light is proportional to absorbed power which, at constant j/Z , scales as $\Delta E = 3.5/1.9 = 1.8$. A ratio of about 4 is obtained² with a P31 scintillator half as thick as the one in Fig. 3. For this case, the relative ΔE is $3.5/0.84 = 4.2$. The P46 data of Fig. 5 yield a ratio of about 4, also consistent with absorbed power since the relative ΔE is $3.5/0.9 = 3.9$. These results suggest that alphas and protons yield equal amount of light in a given scintil-

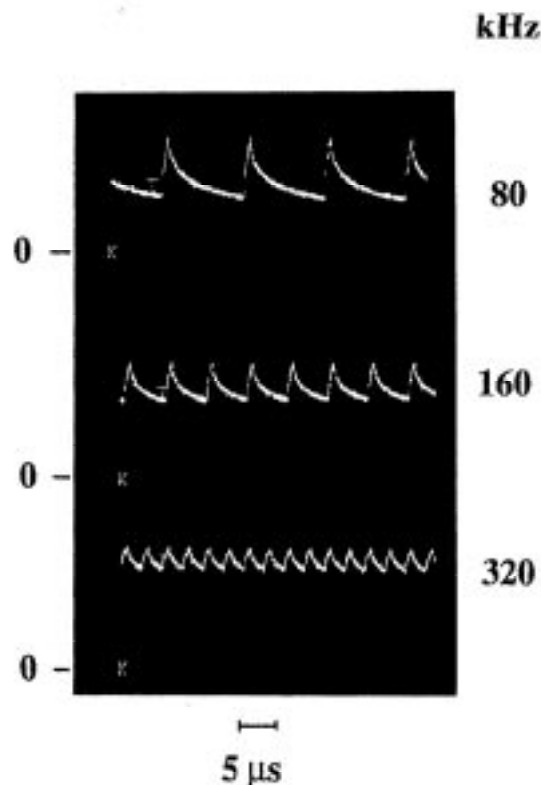


FIG. 7. Response of a P31 scintillator to a chopped 3-MeV proton beam as function of frequency.

lator per unit power deposited within the phosphor powder.

C. Time response

The scintillators must have a fast time response since tokamak instabilities can modulate the detected signals with oscillations in the range 0–1 MHz.¹ A chopper is used to produce Van de Graaf beam current pulses of 1- μ s duration and of 1-nA amplitude at selected time intervals. An example of such a square-pulse train with 12.8- μ s period is shown in Fig. 6(a) from a fast Faraday cup. The responses of the P11 and P31 scintillators to this current waveform have been reported.² The responses of the S2370 and P46 scintillators are shown in Figs. 6(b) and 6(c), respectively.

Typically, a scintillator has a relatively fast rise time and a slower decay time that limits high-frequency resolution. An average $1/e$ decay time τ_d can be obtained from traces such as in Fig. 6. One obtains $\tau_d = \delta / \log(V_M/V_m)$, where δ is the time interval between pulses (11.8 μ s in Fig. 6) and V_M and V_m are the maximum and minimum scintillator amplitudes, respectively. This expression yields τ_d values of about 9 μ s for P11, 18 μ s for P31, 30 μ s for S2370, and 0.1 μ s for P46 scintillators. The ratio V_M/V_m decreases with δ until the modulation disappears, as illustrated in Fig. 7 for the P31 scintillator. A practical upper limit on frequency resolution is about $4/\tau_d$. This limit is

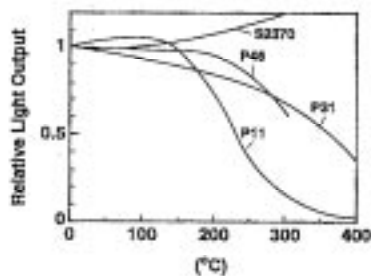


FIG. 8. Relative light output of various scintillators as functions of temperature.

0.44, 0.22, 0.13, and 40 MHz for the P11, P31, S2370, and P46 scintillators, respectively.

D. Temperature dependence and radiation damage

The TFTR scintillator detectors are located very close to the plasma surface, experience high heat loads,³ and must therefore operate at temperatures of up to 300 °C. The relative light outputs of the P11, P31, S2370, and P46 scintillators as functions of temperature are shown in Fig. 8. The P11 and P31 curves come from actual measurements.⁴ The S2370 and P46 curves are reproduced from a Sylvania technical note⁵ and from a journal article,⁶ respectively. All scintillators but the P11 have acceptable light output within the range of temperatures of experimental interest.

The scintillators experience, to various degree, a permanent reduction of their light output from radiation damage.⁷ Energetic ions cause atom displacements and lattice defects in the scintillator powder that promote nonradiative energy losses. Hence, the emitted light decreases as the ionic fluence ($N = \int \Gamma \Delta t$) increases. The cumulative fluence is recorded during the Van de Graaf current scans of Figs. 2–5. From time to time, the light output of the scintillator under study is measured at moderate (10^{-9} – 10^{-8} A/cm²) current densities. Sufficient time intervals are allowed to insure that these measurements are made around room temperature. The relative light outputs of the P11, P31, and P46 scintillators as functions of 3.5-

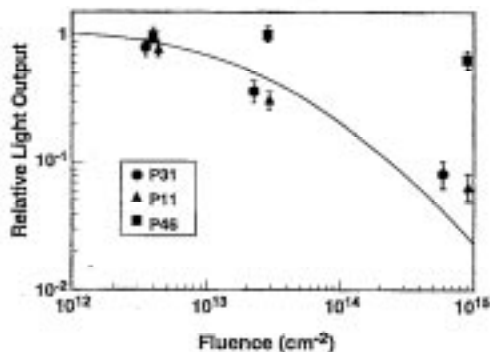


FIG. 9. Relative light output of various scintillators as functions of 3.5-MeV alpha fluence.

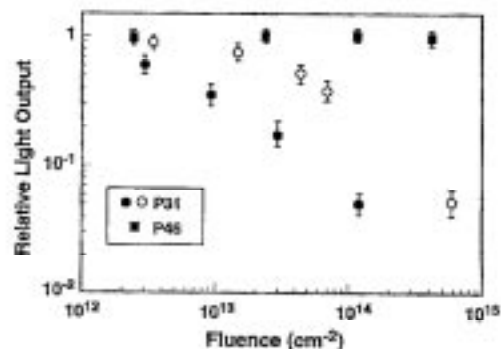


FIG. 10. Relative light output of the P31 and P46 scintillators as functions of fluence. The solid symbols are for 3.5-MeV alphas and the hollow symbols are for 3-MeV protons.

MeV alpha fluence are shown in Fig. 9 with various symbols. The solid line is the empirical expression $(1 + 4 \times 10^{-14} N)^{-1}$ proposed by Brozer and Kallman for ZnS scintillators.⁸ The P11 and P31 data show similar substantial reduction in light output beyond $N \sim 10^{13}$ α/cm², in rough agreement with the empirical expression. On the other hand, the P46 scintillators show little decrease in efficiency up to about 10^{15} α/cm².

Radiation damage can also be observed as function of time at high current densities. The light outputs of the scintillators are recorded as functions of time during exposures of several minutes to steady Van de Graaf beams of 10^{-7} – 10^{-6} A/cm². In some cases, the output decreases significantly after only a few seconds. The relative light outputs of the P31 and P46 scintillators as functions of fluence (time) are shown in Fig. 10. Results similar to those in Fig. 9 are obtained. At a given fluence, the 3.5-MeV alpha damage is substantially larger than the one caused by 3-MeV protons, as expected from the heavier ion mass.⁹ One should note that temperature effects may play some role in the data of Fig. 10 since beam heating is significant at high current densities. For example, a 3-MeV proton beam of 10^{-6} A/cm² current density corresponds to a power density of about 1 W/cm² into a P31 scintillator powder. This results in a temperature rise of about 100 °C, as measured in the back of the quartz substrate with a thermocouple.

III. DISCUSSION

A. Scintillators as fusion product detectors

The ZnS scintillators have been the first choice for the TFTR detectors of escaping charged fusion products because of their high light efficiencies.¹ The results in this article suggest that these scintillators are generally adequate for the D–D experiments performed up to now. In these experiments, 3-MeV protons produce most of the emitted light, with typical fluxes of about 5×10^8 cm⁻² s⁻¹ (MHD instabilities cause occasional flux increases of 3–20) and total fluences of about 10^{12} cm⁻². Hence, ZnS scintillators have a linear response and negligible radiation

damage in these D-D experiments. The P31 scintillator retains high light efficiency at the desired operating temperatures of up to 300 °C. It has a relatively slow time response, but its frequency resolution of up to 0.2 MHz permits detection of most tokamak instabilities.

In future D-T experiments, 3.5-MeV alpha fluxes of up to $5 \times 10^{10} \text{ cm}^{-2} \text{ s}^{-1}$ are anticipated (MHD instabilities may still cause occasional increases of 3–20) and total fluences may reach 10^{13} cm^{-2} . The P31 light output will be sublinear (onset at about $10^{10} \text{ cm}^{-2} \text{ s}^{-1}$) and its light efficiency may decrease by 30% from alpha-induced radiation damage. The data in the article should be useful to account for these effects. The P31 scintillator would be clearly inadequate for future ignited tokamak plasmas. Alpha fluxes of $10^{12} \text{ cm}^{-2} \text{ s}^{-1}$ and fluences of 10^{15} cm^{-2} per ITER¹⁰ discharge are anticipated. The P31 light output would be totally saturated and its light efficiency would decrease by more than one order of magnitude per discharge.

The P46 scintillator appears promising for near-term TFTR D-T experiments and may even prove useful in future ignited plasmas such as in ITER. The P46 is well known in cathodoluminescence applications for its fast time response,¹¹ for its unusually good thermal properties,¹² for its linear light output up to very high excitation densities,^{13,14} and for its exceptional resistance to radiation damage.¹⁵ The P46 data in this article confirm these potential advantages for MeV charged ions: capability of resolving signals of 40-MHz frequency, of operating at temperatures of up to 300 °C, of linear output up to alpha fluxes of at least $5 \times 10^{13} \text{ cm}^{-2} \text{ s}^{-1}$, and of little reduction in light efficiency after alpha fluences of 10^{15} cm^{-2} . However, significant radiation damage would still occur after many ITER-like discharges. In addition, the relatively low P46 light efficiency (0.1 compared to P31) may result in unacceptably low signal-to-noise ratio if parasitic light is substantial. Neutron-induced light from nuclear reactions into the scintillator substrate or into the fiber optics are believed to be the most important sources of parasitic light.¹⁶ In any case, the limiting factor in future ignited plasmas is likely to be fiber optics blackening from radiation damage.¹⁷

The S2370 scintillator does not appear to be as good a choice as the P46 scintillator for tokamak detectors. The S2370 has a rather slow time response, a low light efficiency, and a linear response over a limited range of excitation densities. Other scintillators may prove useful as tokamak detectors of escaping fusion products. For example, the P47 ($\text{Y}_2\text{SiO}_5:\text{Ce}$) and the PX87 ($\text{Y}_3\text{Al}_5\text{O}_{12}:\text{Ga}:\text{Ce}$) are blue-emitting phosphors that have fast time responses and that have light efficiencies larger by factors of 1.4–2.0 compared to P46 scintillators. They may prove good choices if their linearity and radiation resistance are comparable to those of P46 scintillators. Whether to use a green or a blue scintillator might then depend on the origin of neutron-induced fiber optics luminescence, which remains unclear.¹⁷

B. Origin of the ZnS nonlinearities

The saturations of the light emitted by ZnS scintillators at high current densities (see Figs. 2 and 3) are not surprising since luminescence from MeV ions is similar to that from 10–20 keV electrons (cathodoluminescence) where sublinearities are commonly observed. These sublinearities at high electron beam current densities are a serious problem in maintaining color balance of television screens.^{18,19} Sublinearities have also been reported when ZnS scintillators are excited by intense UV light.²⁰ The onsets of saturations occur^{21–23} at power densities of 1–10 mW/cm², similar to those in this article.

In spite of numerous observations over many decades^{22,23} the origin of the above saturations is not completely understood. Traditional hypotheses²¹ include thermal quenching at high temperatures, efficiency decrease through radiation damage, electrical charge effects, and saturation of luminescent centers. The results in this article allow to discard all but the last of these potential causes. The ZnS temperatures cannot increase by more than 10–20 °C from absorbed power densities of 10 mW/cm² and typical fluences of about 10^{12} cm^{-2} are too low to account for the onsets of the saturations.² Some current scans with chopped beams of 10% duty factor show identical saturation onsets as in Figs. 2 and 3. Radiation damage is substantial only at very high (10^{-7} – 10^{-6} A/cm^2) current densities.

Electrical charge build-up on the scintillators is sometimes believed to be the main cause of the observed saturations.²¹ Charges between phosphor powder and quartz substrate are thought to be particularly detrimental.²⁴ Scintillator charging certainly occurs in the experiments reported here. Video recordings show spectacular sparks from the scintillator surface to the aluminum holder at current densities greater than 10^{-8} A/cm^2 . Thin aluminum layers between ZnS powder and quartz or in front of the ZnS powder are effective in eliminating sparks, but they do not appear to modify whatsoever the observed saturations. In addition, one should note that the P46 scintillators have no aluminum layer, show considerable sparking, but remain linear at high currents.

Photoluminescent excitation provides additional indirect evidence that charge effects are not responsible for the observed saturations. The P31 and P46 scintillators are excited by UV light from a 50-W mercury lamp as shown in Fig. 11. The light is filtered (Corning filter 9863), attenuated (Oriel N.D. filter set), and focused on the scintillator oriented at $\phi=45^\circ$. The impacted areas are varied in the range 0.15–1 cm² by changes in the location of the focusing quartz lenses. The relative light outputs of the P31 and P46 scintillators as functions of UV excitation density are shown in Figs. 12 and 13, respectively. The P31 scintillator displays saturations similar to those in Fig. 3 while the P46 remains linear in all cases as in Fig. 5. These and other²⁰ photoluminescent data suggest that the observed saturations are not due to charge effects.

Saturation of luminescent centers has been proposed²⁵ as the cause of scintillator sublinearities. Excitation creates electron-hole pairs in the ZnS powder.¹⁸ Recombination of

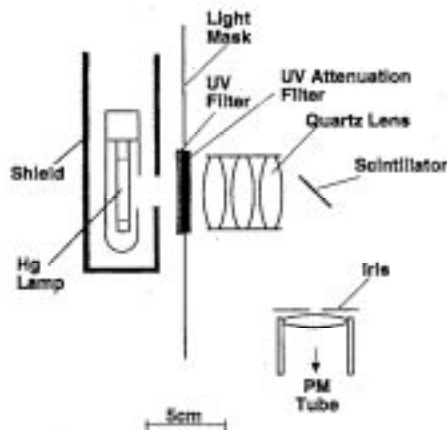


FIG. 11. Apparatus used for photoluminescent experiments.

these pairs excites the activator ions (Ag or Cu). Visible light is emitted when the excited impurities return to ground state. Activator ground-state depletion¹⁹ (also called²² "true activator saturation") can occur at high excitation densities. One can crudely estimate the incident power densities necessary for saturation. The activator surface densities are about 10^{16} cm^{-2} for concentrations of $10^{-4} \text{ g atom per mole ZnS}$ and for thicknesses of $10 \mu\text{m}$. Hence, the maximum excitation rates are $10^{20} \text{ cm}^{-2} \text{ s}^{-1}$ since deexcitation times are 10^{-4} s . Electron-hole pair creation (7.6 eV in ZnS) at such rates would require power densities of 100 W/cm^2 that exceed by four orders of magnitude the power densities at the onset of the saturations. Hence, it appears that true activator saturation is unimportant in the initial part of the observed sublinearities.

Recent cathodoluminescence experiments²³ in which the activator concentration is varied also conclude that the onset of saturations cannot be explained in terms of true activator saturation. Instead, nonradiative (Auger) decay processes appear most likely: when a sufficient density of

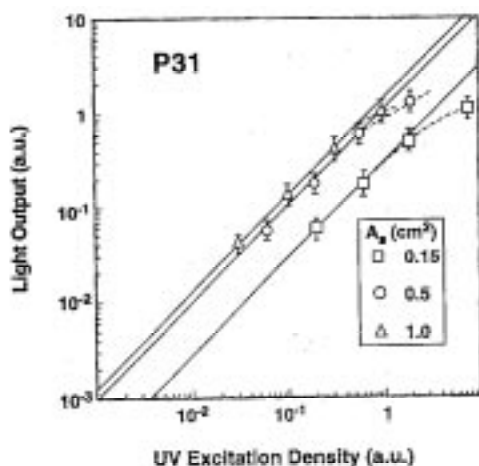


FIG. 12. Light output of a P31 scintillator as function of UV excitation density.

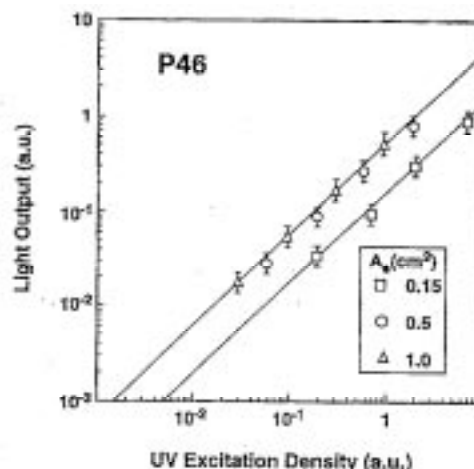


FIG. 13. Light output of a P46 scintillator as function of UV excitation density.

excited activator ions is reached, Coulomb interactions between two or more activator ions can result in deexcitation without visible emission. Such nonlinear losses have been modeled¹³ and found in good agreement with some scintillator sublinearities. A three-center Auger process has been proposed to explain the onsets of saturations in P31 scintillators.²² However, a definitive mode for ZnS scintillators is not yet available and is beyond the scope of the present article.

ACKNOWLEDGMENTS

The authors wish to thank the staff of the Los Alamos Ion Beam Facility for excellent beam operation and Doug Darrow for several useful discussions and scintillator shipping. This work was supported by the U. S. DOE.

¹S. J. Zweben, R. L. Boivin, C. S. Chang, G. W. Hammett, and H. E. Mynick, *Nucl. Fusion* **31**, 2219 (1991).

²M. Tuszewski and S. J. Zweben, *Rev. Sci. Instrum.* **63**, 4542 (1992).

³S. J. Zweben, R. L. Boivin, S. L. Liew, D. K. Owens, J. D. Strachan, and M. Ulrickson, *Rev. Sci. Instrum.* **61**, 3505 (1990).

⁴R. L. Boivin, Z. Lin, L. Roquemore, and S. J. Zweben, *Rev. Sci. Instrum.* **63**, 4418 (1992).

⁵Sylvania technical information bulletin, GTE TIB/107, CM-9199 (1986).

⁶L. A. Bendenskii *et al.*, *Izv. Akad. Nauk SSSR Seria Fiz.* **38**, 1205 (1974).

⁷J. B. Birks, *The Theory and Practice of Scintillation Counting* (Pergamon, New York, 1964).

⁸J. Brozer and H. Kallman, *Z. Naturforsch.* **5a**, 82 (1950).

⁹J. R. Young, *J. Appl. Phys.* **26**, 1302 (1955).

¹⁰K. Tomabechi, J. R. Gilleland, Yu. A. Sokolov, R. Toshi, and the ITER Team, *Nucl. Fusion* **31**, 1135 (1991).

¹¹G. Blasse and A. Brill, *Appl. Phys. Lett.* **11**, 53 (1967).

¹²J. M. Robertson and M. W. van Tol, *Appl. Phys. Lett.* **37**, 471 (1980).

¹³D. M. de Leeuw and G. W't. Hooft, *J. Lumin.* **28**, 275 (1983).

¹⁴W. F. van der Weg and M. W. van Tol, *Appl. Phys. Lett.* **38**, 705 (1981).

¹⁵J. B. Pawley, in *Proceedings of the 7th Annual Scanning Electron Microscopy Symposium*, edited by O. Johari and I. Corin (IIT Research Institute, Chicago, IL, 1974), p. 27.

¹⁶S. J. Zweben, *Rev. Sci. Instrum.* **60**, 576 (1989).

¹⁷A. T. Ramsey and K. W. Hill, *Rev. Sci. Instrum.* **63**, 4735 (1992).

- ¹⁸ L. Ozawa, in *Cathodoluminescence* (VCH, New York, 1990), p. 151.
- ¹⁹ B. G. Yacobi and D. B. Holt, in *Cathodoluminescence Microscopy of Inorganic Solids* (Plenum, New York, 1990), p. 234.
- ²⁰ W. De Groot, *Physica* **6**, 393 (1939).
- ²¹ V. L. Levshin *et al.*, in "Soviet researchers on luminescence," *Transactions of the Lebedev Physics Institute*, edited by Acad. D. V. Skobel'tsyn, (Consultants Bureau, New York, 1964), Vol. 23.
- ²² S. Kuboniwa, H. Kawai, and T. Hoshina, *Jpn. J. Appl. Phys.* **19**, 1647 (1980).
- ²³ W. B. Nottingham, *J. Appl. Phys.* **8**, 877 (1937).
- ²⁴ K. Yanchevskii, *Izv. Akad. Nauk SSSR* **9**, 463 (1945).
- ²⁵ A. Brill, *Physica* **15**, 361 (1949).